

PHYSICAL REVIEW B

CONDENSED MATTER

THIRD SERIES, VOLUME 50, NUMBER 18

1 NOVEMBER 1994-II

Acoustic velocities and refractive index of SiO₂ glass to 57.5 GPa by Brillouin scattering

Chang-sheng Zha, Russell J. Hemley, Ho-kwang Mao, Thomas S. Duffy, and Charles Meade
*Geophysical Laboratory and Center for High Pressure Research, Carnegie Institution of Washington,
5251 Broad Branch Road N.W., Washington, D.C. 20015*

(Received 13 May 1994)

The hypersonic sound velocity and refractive index of SiO₂ glass has been measured to 57.5 GPa at room temperature by Brillouin scattering in diamond cells. On compression, both longitudinal and transverse modes exhibit an anomalous change in slope in the low-pressure region. Between 12 and 23 GPa, the sound velocities increase rapidly. At higher pressures, the bulk velocity follows a trend similar to that expected for coesite. At 57.5 GPa, the longitudinal velocity of SiO₂ glass is 11.85 (±0.51) km/s and the transverse velocity is 6.12 (±0.06) km/s. The refractive index increases monotonically with pressure and reaches a value of 1.924 (±0.081) at 57.5 GPa. It decreases reversibly on decompression to 26 GPa, but displays an irreversible change when decompressed from 16 GPa to ambient pressure. The pressure-density relation calculated from the measured sound velocities within the elastic compression region is in good agreement with several previous determinations.

I. INTRODUCTION

As one of the best-studied amorphous solids, SiO₂ glass has become a prototype system for understanding the disordered state. This tetrahedral random network glass is characterized by a number of anomalous properties. Of particular interest in this regard has been the anomalous behavior of the glass at high pressures. Early high-pressure experiments demonstrated that the equation of state of SiO₂ glass was unusual, exhibiting an initial increase in compressibility with pressure.^{1,2} Further, early studies documented that the material can be irreversibly densified under pressure.^{3,4} Such compaction can be released on heating the recovered material at ambient pressure. The glass can also be densified by shock loading and neutron irradiation (e.g., Ref. 5). Under hydrostatic loading at room temperature, this compaction begins at 8–10 GPa, below which the compression remains elastic. *In situ* vibrational spectroscopic measurements reveal significant changes in structure and dynamics starting as low as a few gigapascals.^{6,7} Large pressured-induced structural changes are also evident from *in situ* x-ray-diffraction measurements.⁸ Because of relaxation effects, the equation of state (as well as other properties) must be characterized by a frequency dependence.⁹ Measurements of the strength of the glass to 60 GPa suggest an increase to ~30 GPa followed by a monotonic decrease.¹⁰

Silica glass (fused silica) and quartz have also been extensively studied by shock wave methods. SiO₂ glass

behaves as a nonlinear elastic solid under shock compression to 9–10 GPa.^{11,12} Recovered samples from shock compression at 10–16 GPa show evidence for permanent densification.¹¹ SiO₂ glass begins to undergo a high-pressure phase transition to a high-density structure at about 16 GPa and this transformation is complete near 30 GPa. At pressures near 70 GPa, discontinuities in shock temperature and sound velocity has been interpreted as shock-induced melting.^{13,14} Above about 30 GPa, the Hugoniot curves of silica glass and quartz overlap, suggesting they both transform to the same high-pressure phase, although the shock temperatures in the two materials are significantly different. The nature of the high-pressure phase formed under shock compression has long been the subject of controversy. While Hugoniot data, release curves, and shock temperatures can all be consistently described by the assumption of transformation to stishovite,^{13,15–17} little or no high-pressure crystalline material is found in shock-recovered samples.¹⁸ The lack of recovered stishovite implies either the formation of a dense, highly coordinated, amorphous phase at high pressure with properties similar to the crystalline form,¹⁸ or formation of disordered material from stishovite at relatively low pressure upon isentropic release.¹⁷

Sound velocity measurements have provided crucial information on the unusual high-pressure behavior of silica glass. Previous work carried out using ultrasonic methods documented a change in pressure dependence of the compressibility (bulk modulus),^{19,20} consistent with the trend observed in the early direct volume measurements of Bridgman.^{1,2} Kondo *et al.*²⁰ found negative

pressure derivatives for both the bulk and shear moduli. Sasakura and co-workers^{21,22} extended the ultrasonic measurements of the glass to 6 GPa. Sound velocity measurements to higher pressures can be carried out with Brillouin scattering techniques in the diamond cell. Indeed, previous Brillouin studies of the glass have confirmed the trends observed in the ultrasonic experiments, and have extended the measurements of sound velocities into the densification regime (> 8 GPa at 300 K).^{23,24} These studies reveal an increase in sound velocities in the recovered densified material. The first measurements, carried out to 18.2 GPa, obtained only Brillouin frequency shifts because the pressure dependence of the refractive index was not known or measured directly.^{24,25} More recently, measurements of sound velocity and refractive index have been carried out to 25 GPa.²⁶

Understanding the microscopic basis for the high-pressure properties of the glass has been the subject of a number of recent studies. The reversible compaction occurring under static pressures above 8–10 GPa is associated with bond breaking of the tetrahedral linkages, but no appreciable changes in Si-atom coordination.⁶ At higher pressures (> 20 GPa), Raman⁶ and infrared⁷ measurements provide evidence for a destabilization of the SiO_4 tetrahedra and an increase in Si coordination number from four to six. This has been confirmed by direct structural measurements of the glass using synchrotron x-ray-diffraction techniques.⁸ The first detailed theoretical study of pressure effects on the glass was that of Woodcock, Angell, and Cheeseman,²⁷ who carried out a molecular-dynamics simulation of structural and dynamical effects associated with densification. There has been renewed theoretical interest in the behavior of the high-density amorphous forms of SiO_2 , including those produced from compression of vitreous (melt-quenched) glass^{28–30} and the disordered material induced from metastable compression of crystalline polymorphs.^{31–36} Specifically, the calculations provide quantitative predictions of changes in short- and intermediate-range order in the material. As a result of the development of increasingly reliable interatomic potentials,^{28,37–39} comparison between theory and experiments provides new insight into the properties of silica glass, and of amorphous states in general.

Further understanding of the high-pressure behavior of the glass requires extending static *in situ* measurements to higher pressures. Recently, we have implemented new techniques for measurements of Brillouin scattering with diamond cells to achieve higher precision and higher pressures than previous work.⁴⁰ We report new results which extend the static pressure range of sound velocity and refractive index measurements as a function of both compression and decompression. We also obtain the pressure-density relation and Poisson's ratio. The results are compared in detail with previous static and dynamic compression data from a variety of experiments as well as with recent theoretical calculations.

II. EXPERIMENTAL TECHNIQUES

Two Brillouin-scattering experiments were performed on polished platelets (~ 10 μm thickness) of Herasil

type-II SiO_2 glass, the same material used in several previous high-pressure studies.^{6–8} One sample was loaded into a large-opening Merrill-Bassett diamond cell and the other into a Mao-Bell-type Brillouin-scattering diamond cell.⁴¹ The former was used to a maximum pressure of 16 GPa with a T-301 stainless-steel gasket, and the latter was used in the pressure interval of 16–57.5 GPa with a rhenium gasket. A 4:1 methanol-ethanol mixture was used as a pressure medium, and the pressure was measured with the ruby fluorescence technique.⁴² The pressure difference between the region sampled by the Brillouin measurements and location of the ruby was estimated to be 1 GPa at the highest pressure. Brillouin spectra were measured with a newly designed system employing a six-path Sandercock-type Fabry-Perot interferometer.^{40,43} To obtain both the longitudinal and transverse sound velocities as well as the refractive index, we used both symmetric 90° and backscattering geometries.^{44,45}

Above 40 GPa, the longitudinal wave of SiO_2 glass overlapped the intense diamond transverse mode; as a result, we obtained only the transverse sound velocities for the glass with the 90° symmetric geometry. This problem was overcome by use of a 135° scattering geometry as shown in Fig. 1. This was then combined with data obtained using a backscattering geometry to invert for the refractive index and the longitudinal sound velocities. For the 135° scattering geometry (Fig. 1), the sound velocity, V , and the half scattering angle, θ , for sample backward scattering are calculated by the following equations:

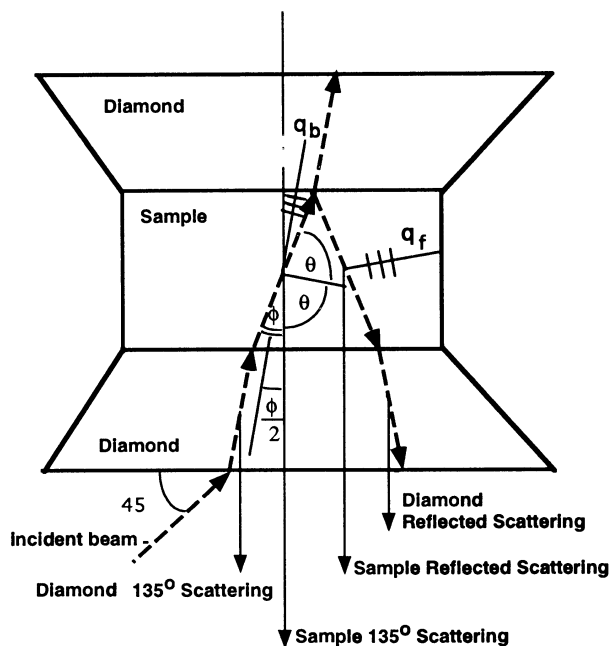


FIG. 1. 135° scattering geometry in the diamond-anvil cell. q_b and q_f are the phonon propagation vectors for backscattering and forward scattering, respectively. The 90° and 180° scattering geometries used in this study are described in Ref. 40.

$$V = \frac{\Delta v_{135} \lambda}{2n \sin \theta} = \frac{\Delta v_{180} \lambda}{2n}, \quad (1)$$

$$\sin \theta = \frac{\Delta v_{135}}{\Delta v_{180}}, \quad (2)$$

where λ is the wavelength of incident beam, n is the refractive index of the sample, Δv_{135} and Δv_{180} are phonon frequency shifts at 135° scattering and backscattering, respectively. The above relations hold only for both optically and elastically isotropic materials as in the case of liquids or glasses. Equation (2) holds only if there is no velocity dispersion. The refractive index is obtained from the relation:

$$n \sin \phi = \sin 45^\circ, \quad (3)$$

where the angle ϕ is given by $\phi/2 + \theta = 90^\circ$. In the present experiments no backscattering data were obtained on compression between 40 and 57.5 GPa because of anomalously strong elastic scattering in this regime. Also, the intensity of the shear mode in this pressure range on compression was relatively low. Measurements were performed on decompression for both the 16- and 57.5-GPa experiments. In the lower-pressure experiment, decompression measurements were carried out to ambient pressure. Decompression measurements from 57.5 GPa were interrupted at 26 GPa because of gasket failure.

III. RESULTS

A. Sound velocities

Figure 2 shows the Brillouin spectra taken at the highest pressure. This example shows that the longitudinal peaks of SiO₂ overlapped the diamond peaks in the 90° geometry, but were well resolved in the 135° scattering configuration. Figure 3 shows the sound velocity of SiO₂ glass as a function of pressure during compression and decompression. All of the velocities were measured with the 90° scattering geometry, which is independent of the refractive index,⁴⁵ except for the longitudinal velocities measured at 57.5 GPa and upon decompression from this pressure which were determined from a combination of 135° scattering and backscattering experiments. Because of the dependence on refractive index, these longitudinal results have larger uncertainties. The uncertainties for the rest of the data of this study are within the size of the points.

At low pressures, the longitudinal and transverse sound velocities of SiO₂ glass are close to those measured by ultrasonic techniques.²⁰ We confirm previous studies in which the glass was found to exhibit an anomalous minima in the longitudinal and transverse velocities around 3 GPa.^{3,20,22–26} On decompression from 16 GPa to ambient conditions, the data show a large irreversible increase in the acoustic velocities. By comparison, there appears to be little hysteresis in the decompression data measured at high pressures (57.5–26 GPa). Also, we find a large increase in the intensity of the shear wave on

decompression from 57.5 GPa. This may be related to time-dependent changes in the sample over the long time scale of this experiment.⁴⁶

Our data are compared with previous Brillouin scattering data in Fig. 4. Polian and Grimsditch²⁶ reported irreversible behavior for both the shear and longitudinal modes upon decompression of the glass from 25 GPa [Fig. 4(a)]. Some discrepancies are observed in the 10–17 GPa region. Differences between our results and those of Schroeder, Dunn, and Bundy²³ may be associated with differences in starting materials. On the other hand, our backscattering data are in good agreement with those of Grimsditch,²⁵ which are shown in Fig. 4(b).

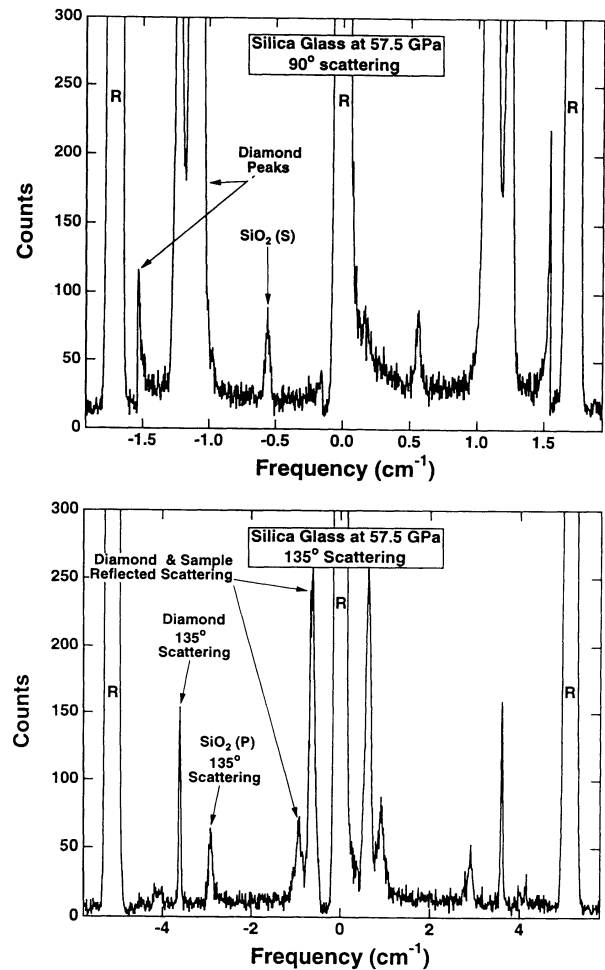


FIG. 2. Brillouin spectra of SiO₂ glass at 57.5 GPa. *R*, *P*, and *S* represent Rayleigh, longitudinal, and transverse peaks, respectively. The free spectral range for 135° scattering is three times larger than that of 90° scattering, and no *S* wave for SiO₂ glass was obtained with 135° scattering because it has low intensity. In the 135° scattering spectrum, the diamond peaks close to the central Rayleigh peak are produced by the laser beam reflected from the diamond culet surfaces at a small scattering angle.

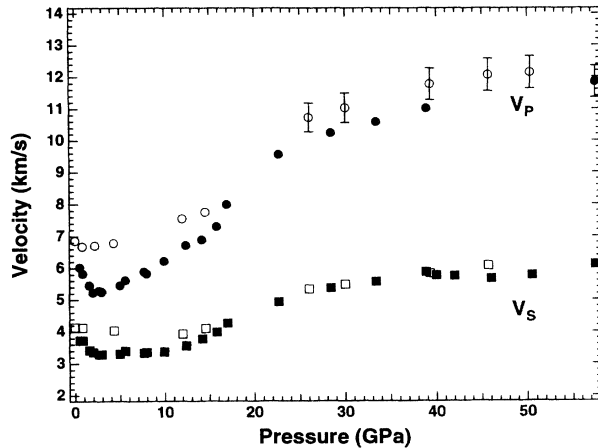


FIG. 3. Sound velocities in SiO_2 glass as a function of pressure. Solid symbols, compression; open symbols, decompression.

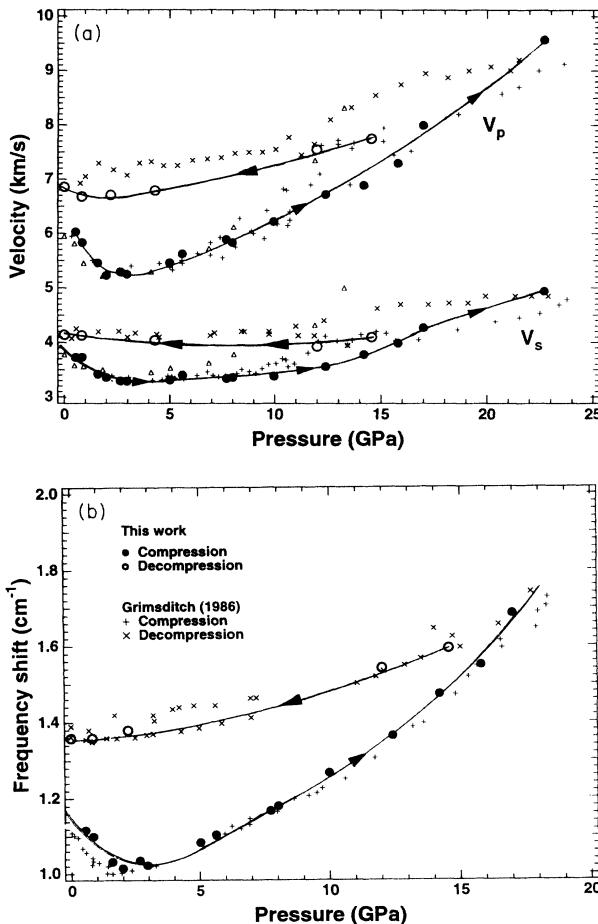


FIG. 4. Comparison of Brillouin data from this study in the lower pressure range and previous work: (a) longitudinal (V_P) and shear (V_S) velocities. Solid circles (compression); open circles (decompression), this study. Pluses (compression) and crosses (decompression), Polian and Grimsditch (Ref. 26). Triangles (compression), Schroeder *et al.* (Ref. 23). (b) Brillouin frequency shifts measured in backscattering mode.

B. Index of refraction

Figure 5 shows the pressure dependence of the refractive index for SiO_2 glass on both compression and decompression. Our results show significantly reduced scatter relative to previous work. Overall, the refractive index of SiO_2 glass increases with pressure. A least-squares fit to the data yields $n = 1.459 + 1.147 \times 10^{-2}P - 6.68 \times 10^{-5}P^2$, where n is refractive index (P is the pressure in GPa). The refractive index of the starting sample was $1.463 (\pm 0.001)$ as determined by the immersion method, and is in excellent agreement with the ambient-pressure value obtained from both the fit and previous data.⁴⁷ On decompression, the index decreases reversibly at high pressures, but is almost flat in the low-pressure region leading to an irreversible increase at ambient pressure. It is believed that the irreversible change of the refractive index must be the result of permanent structural densification. Because the densification process mainly occurs between 10 and 25 GPa (e.g., Ref. 48), the lack of irreversible changes at pressures higher than 26 GPa is perhaps not unexpected.

The densified sample recovered from 16 GPa has a refractive index of 1.528 at ambient pressure; this corresponds to the refractive index at 6.25 GPa during compression. If we assume the densified sample has the same density as that at this pressure during compression, the increase in density is 19.6% above the starting density. This is compared with the results reported by Ref. 49, where a 20% increase in density was measured for a bulk sample recovered from 16 GPa in a large-volume press.

C. Equation of state

Below 8–10 GPa, the compression of SiO_2 glass is elastic under hydrostatic stress (allowing for sufficient relaxation time). We can use the present data to constrain the density of SiO_2 glass from the formula:

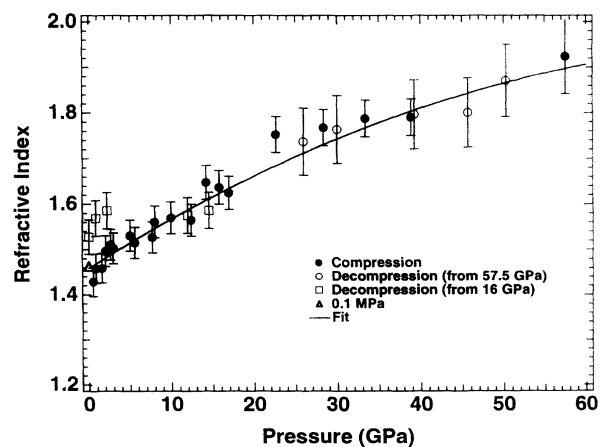


FIG. 5. Pressure dependence of refractive index in SiO_2 glass on compression and decompression. The triangle shows the one-bar refractive index.

$$\rho_P - \rho_0 = \int_{P_0}^P \gamma dP / V_B^2, \quad (4)$$

where ρ_P, ρ_0 are the density of SiO₂ glass at pressure P and ambient pressure P_0 , respectively, V_B is bulk sound velocity, $\gamma = C_p/C_v \approx 1$ is the ratio of the specific heats at constant pressure and volume. For elastically isotropic materials

$$V_B^2 = V_P^2 - 4V_S^2/3, \quad (5)$$

where V_P and V_S are longitudinal and transverse sound velocities. The calculated densities as a function of pressure are compared with previous static compression data^{2,9,22,23} (Fig. 6). The recent ultrasonic determination of Suito *et al.*²² to 8 GPa is close to the present results. Above 10 GPa, the compression properties of SiO₂ glass show irreversible effects, with structural relaxation and densification occurring.^{3,6,8,9,24,25,50} In this range, it is necessary to use a relaxed sound velocity which may differ significantly from that measured by Brillouin scattering (e.g., Ref. 51).

From the refractive index and density to 10 GPa, we can calculate the polarizability of SiO₂ glass from the Lorentz-Lorenz equation:

$$\frac{n^2 - 1}{n^2 + 2} = \frac{4}{3} \pi \alpha \frac{N}{V}, \quad (6)$$

where α , N , and V are the polarizability, Avogadro's number, and molar volume, respectively. The results are shown in Fig. 7, which shows the polarizability of SiO₂ glass decreases with pressure on elastic compression.

D. Poisson's ratio

Poisson's ratio, σ , is obtained directly from the measured sound velocities by the equation,

$$\sigma = \frac{V_P^2 - 2V_S^2}{2(V_P^2 - V_S^2)}. \quad (7)$$

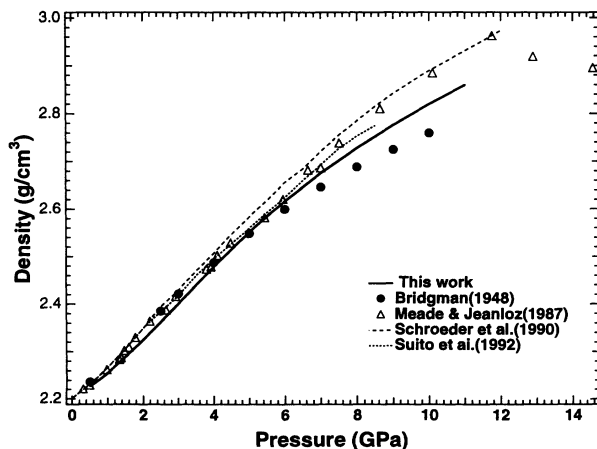


FIG. 6. Comparison of pressure-density relation for SiO₂ glass in the elastic compression regime with those determined by static compression experiments.

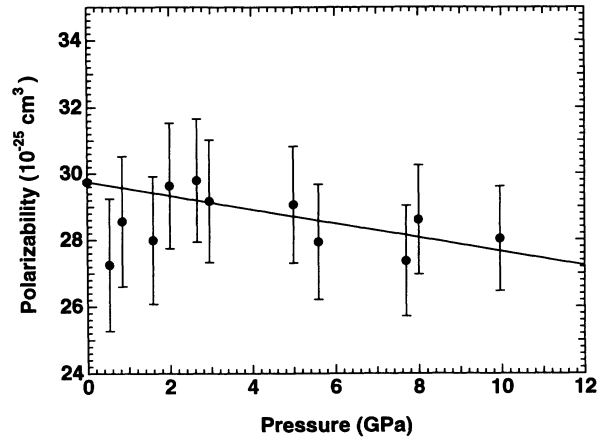


FIG. 7. Pressure dependence of polarizability for SiO₂ glass within the elastic compression region.

As shown in Fig. 8, the measured values start from 0.19 at 0.54 GPa, decrease to ~ 0.15 , then increase to about 0.30–0.35, becoming nearly pressure independent above 23 GPa. For most metals, σ is between 0.25 and 0.35, and the value for a liquid is 0.5. SiO₂ glass is less ductile at low pressures. With increasing pressure, the ductility of the glass is close to typical values for metals. The evidence for increasingly ductility of amorphous silica with pressure above ~ 30 GPa is thus consistent with the reported decrease in shear strength at these pressures.¹⁰

IV. DISCUSSION

In general, we find that the longitudinal sound velocities are more sensitive to changes in pressure than the transverse velocities. Overall, the largest changes in the sound velocities occur between 12 and 23 GPa. We interpret this change as arising from permanent densification.⁴⁸ At this pressure, the gradual increase in

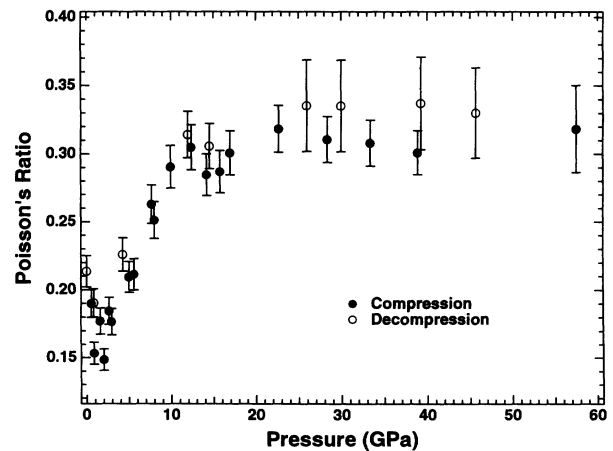


FIG. 8. Poisson's ratio of SiO₂ glass as a function of pressure. Solid circles are increasing pressure and open circles are on decreasing pressure.

Si coordination observed by x-ray diffraction begins.⁸ Over the entire pressure range studied, the longitudinal sound velocity changes by more than a factor of 2, while the transverse sound velocity changes by somewhat less than this factor.

Our longitudinal velocity at the highest pressure is 11.85 km/s, which is close to that of stishovite at ambient pressure, whereas the transverse velocity is lower than that of stishovite at ambient pressure.⁵² Thus, the sound velocity of SiO₂ glass at the highest pressure of this study is presumably much lower than stishovite at the same pressure. Figure 9 shows the bulk sound velocities of SiO₂ glass and possible aggregate sound velocities of quartz and coesite at high pressure which were constrained from the static compression data published in Ref. 32. It is of interest to note that the bulk sound velocity profile of glass is within the range of that expected for coesite above 23 GPa. We note, however, that this is an extrapolated curve and that coesite undergoes a phase transition and becomes amorphous in this higher range.^{31,32} Nevertheless, the velocities in the glass lie well below those expected for six-coordinated crystalline SiO₂. Bridgman and Simon³ reported that the densified glass was anisotropic as a result of the uniaxial component of the stress. At the highest pressures (e.g., 57.5 GPa) our sample also experienced nonhydrostatic pressures, and we therefore expect elastic (and structural) anisotropy exists in our samples quenched from these conditions.⁵³

Sound velocities for quartz and silica glass have been reported under shock compression to pressures between 8 and 147 GPa.^{14,54–57} These are compared to the present data for silica glass in Fig. 10. In the low-pressure and transformation regions (below 40 GPa), the Hugoniot sound velocities in quartz and silica glass are comparable to 300-K compressional and bulk sound velocities of silica glass at these pressures. In the high-pressure region, there are considerable differences in Hugoniot sound velocities reported in different studies for quartz starting

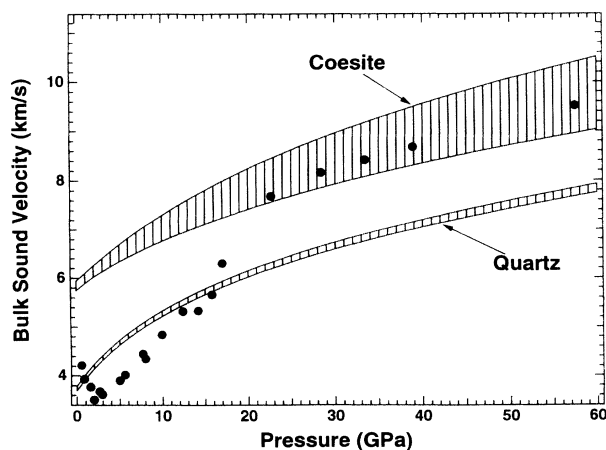


FIG. 9. Pressure dependence of bulk sound velocity for SiO₂ glass, quartz, and coesite. Solid symbols, SiO₂ glass (this study).

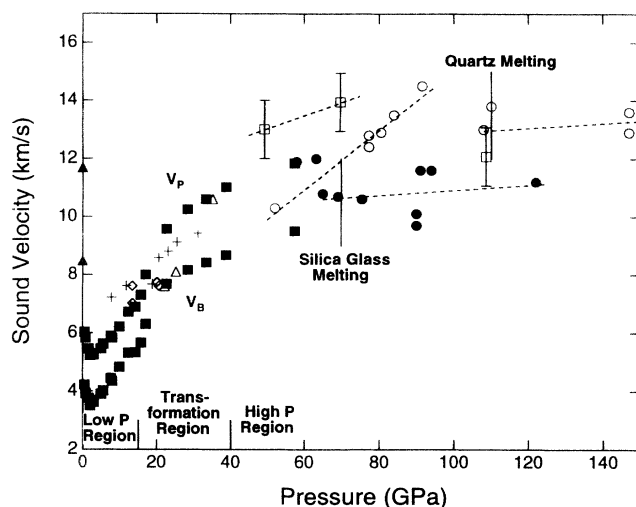


FIG. 10. Sound velocities in silica glass and quartz under shock compression compared with compressional and bulk velocities under static compression (solid squares). The vertical lines at 70 and 110 GPa show the approximate location of melt boundaries under shock compression for silica glass and quartz, respectively. Hugoniot data for silica glass are shown by the solid circles (Ref. 14) and diamonds (Ref. 56), other symbols are for quartz starting material (pluses) (Ref. 55); open triangles (Ref. 54); open squares (Ref. 57); open circles (Ref. 14). Dashed lines serve to connect different data sets at high pressure. The solid triangles show the ambient pressure (0.1 MPa) compressional and bulk sound velocities for stishovite (Ref. 52).

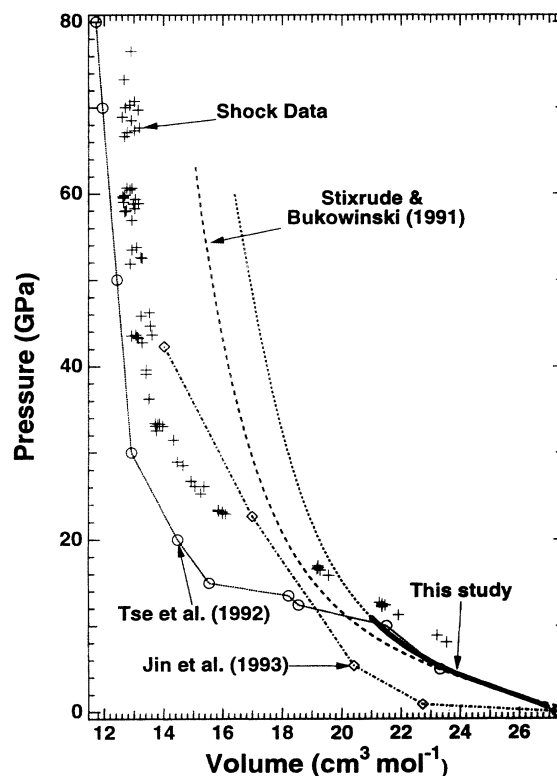


FIG. 11. Pressure-volume relations for SiO₂ glass, including the results of the present study extrapolated to higher pressures, shock-wave results (Ref. 60), and theoretical calculations.

material. The measured compressional velocity at 57.5 GPa in this study is very similar to that reported in silica glass shocked to 58 GPa.¹⁴ The shock temperature in SiO₂ glass at 59 GPa is 4950 K.¹³ At about 70 GPa for silica glass and about 110 GPa for quartz, the sound velocities decrease and abrupt changes in emitted thermal radiation are observed; both these phenomena are consistent with shock-induced melting.¹³ Above these pressures, the measured Hugoniot velocity corresponds to the bulk sound speed. The Hugoniot sound velocities in silica glass above the melting point are broadly consistent with the trend defined by the measured bulk sound velocities of this study. Thus, within the pressure regime of the shock-induced high-pressure phase of silica glass, compressional and bulk sound velocities appear to be similar under both static and dynamic loading, despite temperature differences of 4500 K or more.

We compare the pressure-volume relations determined from the present study with theoretical calculations (Fig. 11). As discussed above the comparison is strictly valid only below 10 GPa, where relaxation effects are not appreciable. In this pressure range, the calculations of Tse *et al.*²⁹ are particularly close to the experimental curve. These calculations were carried out using the effective two-body potential of van Beest, Kramer, and van Santen,³⁸ which is similar to that proposed by Tsuneyuki *et al.*³⁷ The calculations predict a large volume collapse beginning at ~10 GPa, which results from the pressure-induced 4–6 Si-atom coordination change. A coordination change is also responsible for the volume collapse predicted by Jin *et al.*³⁹ The results of Stixrude and Bukowski²⁸ are also close to experimental curve in the elastic compression regime. The potential used in these calculations requires the SiO₄ tetrahedra to be maintained over the entire pressure range (i.e., no coordina-

tion change is allowed). The experimental curve extrapolated into the densification region follows the trend predicted in Ref. 28. As discussed above, experiments document that the coordination change is spread out over a wide pressure interval.⁸ Further, it is important to emphasize that there is spectroscopic evidence for the persistence of some SiO₄ tetrahedra to ~20 GPa, although at higher pressures the population of tetrahedral groups decreases.⁶ The spectroscopic evidence for the persistence of the tetrahedra to high pressure may therefore be consistent with the closeness of the bulk sound velocity profile of the glass to that calculated for coesite. There is also evidence from vibrational spectra for tetrahedral Si at pressures well above 20 GPa when lower-pressure crystalline phases (e.g., α -quartz) are compressed to pressures well beyond their stability fields.³³

In conclusion, we suggest that there are a variety of metastable states—and a range of Si coordinations—available to the amorphous solid at high pressures which may be accessed by different pressure-temperature-time paths. We further speculate that these states include crystalline approximants (i.e., poorly crystallized or disordered crystalline phases). Indeed, the extent to which the high-density amorphous material resembles stishovite (or its closely related higher-pressure orthorhombic form^{58,59}) remains an open question for further experimental study.

ACKNOWLEDGMENTS

We thank R. E. Cohen and L. Stixrude for useful discussions and correspondence. This work was supported by the NSF. The Center for High-Pressure Research is a NSF Science and Technology Center.

¹P. W. Bridgman, *Am. J. Sci.* **10**, 359 (1925); **237**, 7 (1939).

²P. W. Bridgman, *Proc. Am. Acad. Arts Sci.* **76**, 55 (1948).

³P. W. Bridgman and I. Simon, *J. Appl. Phys.* **24**, 405 (1953).

⁴R. Roy and H. M. Cohen, *Nature* **190**, 798 (1961).

⁵W. Primak, *Compacted States of Vitreous Silica—Studies of Radiation Effects in Solids* (Gordon and Breach, New York, 1975).

⁶R. J. Hemley, H. K. Mao, P. M. Bell, and B. O. Mysen, *Phys. Rev. Lett.* **57**, 747 (1986).

⁷Q. Williams and R. Jeanloz, *Science* **239**, 902 (1988); Q. Williams, R. J. Hemley, M. Kruger, and R. Jeanloz, *J. Geophys. Res.* **98**, 22 157 (1993).

⁸C. Meade, R. J. Hemley, and H. K. Mao, *Phys. Rev. Lett.* **69**, 1387 (1992).

⁹C. Meade and R. Jeanloz, *Phys. Rev. B* **35**, 236 (1987).

¹⁰C. Meade and R. Jeanloz, *Science* **241**, 1072 (1988).

¹¹J. Wackerle, *J. Appl. Phys.* **33**, 922 (1962).

¹²L. M. Barker and R. E. Hollenbach, *J. Appl. Phys.* **41**, 4208 (1970).

¹³G. A. Lyzenga, T. J. Ahrens, and A. C. Mitchell, *J. Geophys. Res.* **88**, 2431 (1983).

¹⁴R. G. McQueen, in *Shock Compression of Condensed Matter-*

1991, edited by S. C. Schmidt, R. D. Dick, J. W. Forbes, and D. G. Tasker (Elsevier, New York, 1992), p. 75.

¹⁵H. Tan and T. J. Ahrens, *J. Appl. Phys.* **67**, 217 (1990).

¹⁶J. Boettger, *J. Appl. Phys.* **72**, 5500 (1992).

¹⁷T. Sekine, T. S. Duffy, A. M. Rubin, W. W. Anderson, and T. J. Ahrens, *Geophys. J. Int.* (to be published).

¹⁸A. J. Gratz, W. J. Nellis, J. M. Christie, W. Brocious, J. Swegle, and P. Cordier, *Phys. Chem. Miner.* **19**, 267 (1992).

¹⁹E. H. Borgadus, *J. Appl. Phys.* **36**, 2504 (1965).

²⁰K.-I. Kondo, S. Ito, and A. Sawaoka, *J. Appl. Phys.* **52**, 2826 (1981).

²¹T. Sasakura, K. Suito, and H. Fujisawa, in *High Pressure Science and Technology*, edited by N. V. Novikov and Y. M. Chistyakov (Naukova Dumka, Kiev, 1989), p. 60.

²²K. Suito, M. Miyoshi, T. Sasakura, and H. Fujisawa, in *High-Pressure Research: Application to Earth and Planetary Sciences*, edited by Y. Syono and M.H. Manghnani (Terra Scientific-Tokyo, American Geophysical Union, Washington, D.C., 1992), p. 219.

²³K. Schroeder, K. J. Dunn, and F. Bundy, in *High Pressure in Research and Industry*, Proceedings of the 8th AIRAPT Conference, edited by C. K. Blackman, T. Johannison, and

- L. Tegner (Arkitektkopia, Uppsala, Sweden, 1982), p. 259.
- ²⁴M. Grimsditch, *Phys. Rev. Lett.* **52**, 2379 (1984).
- ²⁵M. Grimsditch, *Phys. Rev. B* **34**, 4372 (1986).
- ²⁶A. Polian and M. Grimsditch, *Phys. Rev. B* **47**, 13 979 (1993).
- ²⁷L. V. Woodcock, C. A. Angell, and P. A. Cheeseman, *J. Chem. Phys.* **65**, 1565 (1976).
- ²⁸L. Stixrude and M. S. T. Bukowinski, *Phys. Rev. B* **44**, 2523 (1991).
- ²⁹J. S. Tse, D. D. Klug, and Y. L. Page, *Phys. Rev. B* **46**, 5933 (1992).
- ³⁰M. S. Somayazulu, S. M. Sharma, N. Garg, S. L. Chaplot, and S. K. Sikka, *J. Phys. C* **65**, 6345 (1993).
- ³¹R. J. Hemley, in *High-Pressure Research in Mineral Physics*, edited by M. H. Manghnani and Y. Syono (Terra Scientific-Tokyo, AGU-Washington, D.C., 1987), p. 347.
- ³²R. J. Hemley, A. P. Jephcoat, H. K. Mao, L. C. Ming, and M. H. Manghnani, *Nature* **334**, 52 (1988).
- ³³K. J. Kingma, C. Meade, R. J. Hemley, H. K. Mao, and D. R. Veblen, *Science* **259**, 666 (1993); K. J. Kingma, R. J. Hemley, H. K. Mao, and D. R. Veblen, *Phys. Rev. Lett.* **70**, 3927 (1993).
- ³⁴J. S. Tse and D. D. Klug, *Phys. Rev. Lett.* **67**, 3559 (1991).
- ³⁵N. Binggeli and J. R. Chelikowsky, *Phys. Rev. Lett.* **69**, 2220 (1992); N. Binggeli, J. R. Chelikowsky, and R. M. Wentzcovitch, *Phys. Rev. B* **49**, 9336 (1994).
- ³⁶M. S. Somayazulu, S. M. Sharma, and S. K. Sikka, *Phys. Rev. Lett.* **73**, 98 (1994).
- ³⁷S. Tsuneyuki, Y. Matsui, H. Aoki, and M. Tsukada, *Phys. Rev. Lett.* **61**, 869 (1988).
- ³⁸B. W. van Beest, G. J. Kramer, and R. A. van Santen, *Phys. Rev. Lett.* **64**, 1955 (1990).
- ³⁹W. Jin, R. K. Kalia, P. Vashishta, and J. P. Rino, *Phys. Rev. Lett.* **71**, 3146 (1993).
- ⁴⁰C. S. Zha, T. S. Duffy, H. K. Mao, and R. J. Hemley, *Phys. Rev. B* **48**, 9246 (1993); T. S. Duffy, W. Vos, C. S. Zha, R. J. Hemley, and H. K. Mao, *Science* **263**, 1590 (1994).
- ⁴¹H. K. Mao and P. M. Bell, *Carnegie Inst. Washington Yearb.* **79**, 411 (1980).
- ⁴²H. K. Mao, J. Xu, and P. M. Bell, *J. Geophys. Res.* **91**, 4673 (1986).
- ⁴³R. Mock, B. Hillebrands, and J. R. Sandercock, *J. Phys. E* **20**, 656 (1987).
- ⁴⁴H. Shimizu, E. M. Brody, H. K. Mao, and P. M. Bell, *Phys. Rev. Lett.* **47**, 128 (1981).
- ⁴⁵A. Polian, in *Frontiers of High Pressure Research*, edited by H. D. Hochheimer and R. D. Etters (Plenum, New York, 1991), p. 181.
- ⁴⁶This sample was held at the highest pressures for 43 days before it was decompressed, whereas the measurements on compression were performed during a period of 44 days. The higher intensity of the shear wave measured on decompression (which took 18 days) could have been caused by annealing of the sample or relaxation of non-hydrostatic stress while at the highest pressures.
- ⁴⁷R. B. Sosman, *The Phases of Silica* (Rutgers University Press, New Brunswick, NJ, 1965).
- ⁴⁸A. Polian and M. Grimsditch, *Phys. Rev. B* **41**, 6086 (1990).
- ⁴⁹S. Susman, K. J. Volin, D. L. Price, M. Grimsditch, J. P. Rino, R. K. Kalia, P. Vashishta, G. Gwanmesia, Y. Wang, and R. C. Liebermann, *Phys. Rev. B* **43**, 1194 (1991).
- ⁵⁰J. Arndt, *Phys. Chem. Glasses* **24**, 104 (1983).
- ⁵¹G. H. Wolf, S. Wang, C. A. Herbst, D. J. Durben, W. F. Oliveer, Z. C. Kang, and K. Halverson, in *High Pressure Research in Mineral Physics: Applications to Earth and Planetary Sciences*, edited by Y. Syono and M. H. Manghnani (Terra Scientific-Tokyo, American Geophysical Union-Washington, D.C., 1992), p. 503.
- ⁵²D. J. Weidner, J. D. Bass, A. E. Ringwood, and W. Sinclair, *J. Geophys. Res.* **87**, 4740 (1982).
- ⁵³This possibility should be examined in future work. Unfortunately, because this experiment was terminated abruptly at 26 GPa on decompression (see text), we were unable to determine the anisotropy of the sample at ambient pressure.
- ⁵⁴D. E. Grady, W. J. Murri, and P. S. DeCarli, *J. Geophys. Res.* **80**, 4857 (1975).
- ⁵⁵M. N. Pavlovskii, *Z. Prik. Mek. Tek.* **17**, 136 (1976).
- ⁵⁶L. C. Chhabildas and D. E. Grady, in *Shock Waves in Condensed Matter*, edited by J. R. Asay, R. A. Graham, and G. K. Straub (Elsevier, New York, 1983), p. 176.
- ⁵⁷L. C. Chhabildas and J. M. Miller, Sandia National Laboratory Report No. SAND85-1092, 1985.
- ⁵⁸Y. Tsuchida and T. Yagi, *Nature* **340**, 217 (1989).
- ⁵⁹K. J. Kingma, R. E. Cohen, R. J. Hemley, and H. K. Mao, *Eos Trans. Am. Geophys. Union* **74**, 676 (1993).
- ⁶⁰S. P. Marsh, *LASL Shock Hugoniot Data* (University of California Press, Berkeley, 1980).